

# Forecasting When to Forecast: Accelerating Diffusion Models with Confidence-Gated Taylor

Xiaoliu Guan<sup>1,2</sup>      Lielin Jiang<sup>2</sup>      Hanqi Chen<sup>2,3</sup>      Xu Zhang<sup>2</sup>      Jiaxing Yan<sup>2</sup>  
 Guanzhong Wang<sup>2</sup>      Yi Liu<sup>2</sup>      Zetao Zhang<sup>4,\*</sup>      Yu Wu<sup>1,\*</sup>

<sup>1</sup>School of Computer Science, Wuhan University

<sup>2</sup>PaddlePaddle Team, Baidu Inc

<sup>3</sup>International Joint Innovation Center, The Electromagnetics Academy at Zhejiang University

<sup>4</sup>Yunnan Key Laboratory of Media Convergence

{liuxiaoguan, wuyucs}@whu.edu.cn 22360175@zju.edu.cn zzt@yndaily.com  
 {jianglielin, zhangxu44, yanjiaxing, wangguanzhong, liuyi22}@baidu.com

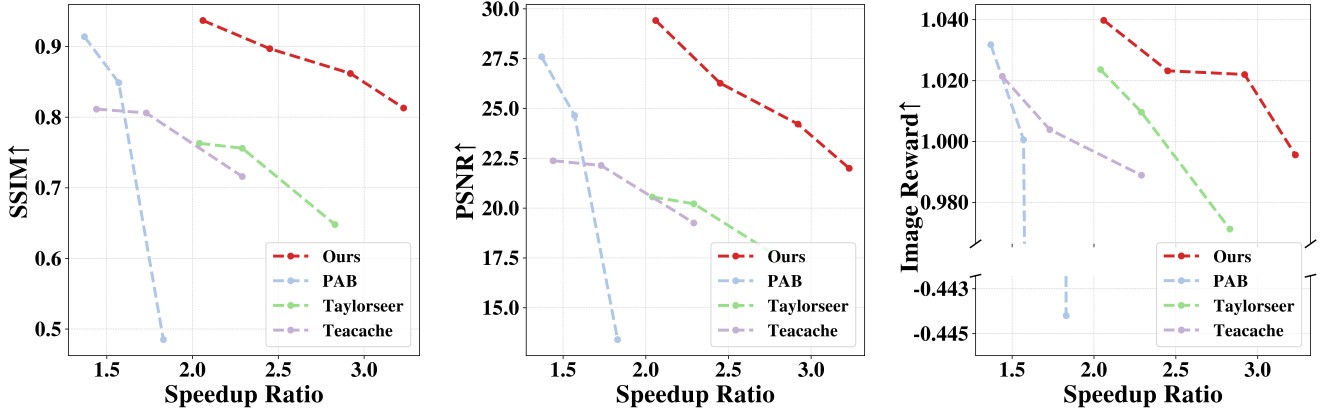


Figure 1. Comparison of our method and baselines under different speedup ratios.

## Abstract

Diffusion Transformers (DiTs) have demonstrated remarkable performance in visual generation tasks. However, their low inference speed limits their deployment in low-resource applications. Recent training-free approaches exploit the redundancy of features across timesteps by caching and reusing past representations to accelerate inference. Building on this idea, TaylorSeer instead uses cached features to predict future ones via Taylor expansion. However, its module-level prediction across all transformer blocks (e.g., attention or feedforward modules) requires storing fine-grained intermediate features, leading to notable memory and computation overhead. Moreover, it adopts a fixed caching schedule without considering the varying accuracy of predictions across timesteps, which can lead to degraded outputs when prediction fails. To address these limitations, we propose a novel approach to better leverage Taylor-based acceleration. First, we shift the Taylor prediction

target from the module level to the last block level, significantly reducing the number of cached features. Furthermore, observing strong sequential dependencies among Transformer blocks, we propose to use the error between the Taylor-estimated and actual outputs of the first block as an indicator of prediction reliability. If the error is small, we trust the Taylor prediction for the last block; otherwise, we fall back to full computation, thereby enabling a dynamic caching mechanism. Empirical results show that our method achieves a better balance between speed and quality, achieving a 3.17x acceleration on FLUX, 2.36x on DiT, and 4.14x on Wan Video with negligible quality drop. The Project Page is [here](#).

## 1. Introduction

In recent years, diffusion models [6, 29, 31] have become foundational to visual generation, owing to their impressive ability to produce high-quality and semantically rich images. Initially built upon U-Net [26] architectures,

\*Corresponding author.

these models have demonstrated strong performance across domains, including text-to-image generation, inpainting, and video synthesis [1, 7, 12, 24, 27, 35, 39]. More recently, the introduction of Diffusion Transformers (DiT) [23] has further advanced scalability and performance, enabling diffusion models to tackle complex generative scenarios and large-scale data [20, 34, 38, 40, 45, 48]. However, despite these advantages, the inherently iterative nature of the denoising process results in low inference speed. This limitation poses a significant challenge for deploying such models in low-resource or latency-sensitive applications. To address the inefficiency of diffusion inference, a variety of approaches have been proposed, reducing the number of sampling steps, such as designing advanced probabilistic-flow-inspired solvers based on Ordinary Differential Equations (ODEs) [17, 18, 44]. Other approaches focus on compressing model size by leveraging techniques like network pruning [46], knowledge distillation [11], and token reduction [3, 9, 41]. However, most of these methods require additional training or offline optimization, introducing extra computational costs and limiting the overall deployment flexibility.

A recent line of work [2, 19, 28, 49, 50] explores the feature redundancy inherent in diffusion models. Based on the observation that features across adjacent steps often exhibit high similarity, these approaches aim to accelerate inference by reusing features from previous timesteps. By caching and reusing past representations instead of recomputing them, these methods significantly reduce computational overhead without any additional training effort. Nevertheless, as the gap between timesteps increases, the assumption of feature similarity gradually breaks down. Naively reusing cached features across distant steps can result in substantial errors, ultimately degrading image quality. To mitigate this, TaylorSeer [15] proposed to predict features at future timesteps using Taylor series expansion based on previously cached features, rather than directly reusing them. This enables the model to retain high generation quality, even under aggressive acceleration.

While TaylorSeer improved the reliability of cached features by predicting future representations through Taylor expansion, it introduces considerable memory overhead and additional latency. Specifically, it applied Taylor expansion at every module within each transformer block (e.g., attention or feedforward module), predicting the residual branch in a step-by-step manner. However, modern diffusion transformer architectures consist of numerous modules, each requiring its own cached features. This design significantly increases memory consumption and computational burden, partially offsetting the intended acceleration gains. To address this issue, we propose a **Last Block Forecast** strategy that reduces memory usage with minimal impact on acceleration performance. TaylorSeer revealed that intermedia-

ate features across blocks are highly predictable. Given the strictly sequential nature of DiT, where each block passes information to the next, we propose to forecast only the last block’s output, which corresponds to the model output at the current timestep. By doing so, we obtain an accurate approximation of the last block output while avoiding the need to cache every module’s residual branch. This strategy requires storing only a single set of features and eliminates much of the computational overhead.

Meanwhile, TaylorSeer adopted a fixed caching schedule by dividing the inference process into equally spaced intervals, computing one feature per interval and using Taylor expansion to predict the remaining ones. This design implicitly assumes that Taylor prediction remains consistently reliable across timesteps, which often does not hold. In practice, the model’s output exhibits dynamic changes, leading to fluctuations in approximation accuracy over time. As a result, a rigid reuse pattern may either miss opportunities for further acceleration or incur significant errors when prediction fails. This limitation raises a natural and important question: *When is the Taylor predictor reliable enough to replace actual computation?*

Intuitively, we only want to rely on the Taylor predictor when it is sufficiently accurate; otherwise, we fall back to the standard full computation. However, evaluating the full computation output just to compare with the predicted result defeats the purpose of acceleration. To address this, we propose a **Prediction Confidence Gating (PCG)** mechanism. Our core hypothesis is that Transformer-based architectures like DiT exhibit strong sequential dependencies. In other words, the quality of early block predictions can reflect the predictability of later ones. Good predictions on early blocks suggest high reliability when forecasting the last block output. Based on this insight, we use the prediction error of the first block as a proxy to assess the confidence of the Taylor prediction at the current timestep. Concretely, we compute the first block’s true output at each timestep and apply Taylor expansion to predict it in parallel. If the predicted result closely matches the ground truth, we consider the model state to be sufficiently stable and apply Taylor approximation for the remaining computation. Otherwise, we fall back to full computation to avoid quality degradation. This approach maintains decision quality while incurring almost no additional computational cost, enabling a training-free, dynamic acceleration strategy.

Our method achieves up to a 3.17x acceleration on the FLUX model, 4.14x speedup on Wan Video, and 2.36x acceleration on DiT, with negligible degradation in image quality. Moreover, compared to TaylorSeer, our approach improves SSIM by approximately 25.5% while being over one second faster, demonstrating a significantly better trade-off between efficiency and fidelity, as shown in Figure 1.

## 2. Related Work

### 2.1. Diffusion Transformer

Diffusion models [6, 29] have achieved remarkable success in content generation, producing high-quality and diverse outputs. Early approaches [24, 25, 27, 36] were predominantly based on U-Net architectures, which delivered strong performance in both image and video generation. However, their scalability is fundamentally limited, posing challenges for building large-scale, high-capacity models. To address this limitation, the Diffusion Transformer (DiT) [23] architecture was proposed, leveraging the scalability and modeling flexibility of Transformers. This shift has led to a wave of progress across various generative tasks. Nonetheless, the broader adoption of DiT remains constrained by the inherently iterative nature of the diffusion process, which significantly hampers inference efficiency.

### 2.2. Diffusion Model Acceleration

With the growing deployment of diffusion models in real-world applications, improving their inference efficiency has become an increasingly important research direction. A variety of methods have been proposed to accelerate the sampling process, which can generally be categorized into three main paradigms.

First, several works aim to shorten the sampling trajectory [32]. For example, methods like DDIM [30] reformulate the generative process to avoid long iterative updates, while others draw inspiration from numerical solvers to make the generation process more efficient. Second, model compression and quantization techniques have been explored to reduce computational overhead, including knowledge distillation [11], token reduction [3, 9, 41], and network pruning [46, 47]. However, these methods often require additional training or offline optimization, which introduces extra computational cost. Third, a growing body of work focuses on training-free acceleration via feature reuse [2, 19, 28, 49, 50], which has gained increasing attention due to its simplicity and effectiveness. These methods are motivated by the observation that intermediate features in diffusion models often contain redundancy, making it feasible to reuse them rather than recomputing at every step. For instance, PAB [43] and T-Gate [14] selectively reuse cached features based on different types of attention. TeaCache [13] proposes an adaptive caching strategy based on timestep-aware differences in output features. TaylorSeer [15] reduces the accumulation of cache reuse errors at distant timesteps by using Taylor expansion to predict feature values. Building upon TaylorSeer, our method further improves prediction utility by explicitly evaluating the reliability of the Taylor approximation at each step. This enables a more principled decision on the predictability of

a timestep, leading to a better trade-off between generation quality and inference efficiency.

## 3. Method

### 3.1. Preliminary

**Diffusion Models.** Diffusion models generate data by learning to reverse a predefined noising process. The forward process gradually corrupts a clean sample  $\mathbf{x}_0$  into a sequence of noisy latents  $\mathbf{x}_1, \dots, \mathbf{x}_T$  by adding Gaussian noise at each timestep. The forward process is defined as:

$$q(\mathbf{x}_t \mid \mathbf{x}_0) = \mathcal{N}(\mathbf{x}_t; \sqrt{\alpha_t} \mathbf{x}_0, (1 - \alpha_t)\mathbf{I}), \quad (1)$$

where  $\alpha_t \in [0, 1]$  represents the noise level. This formulation allows sampling  $\mathbf{x}_t$  directly from  $\mathbf{x}_0$  without computing intermediate steps. To generate new samples, the reverse process aims to recover  $\mathbf{x}_0$  from pure noise  $\mathbf{x}_T$  by iteratively denoising. This is achieved by training a neural network  $\epsilon_\theta(\mathbf{x}_t, t)$  to predict the noise added at each timestep. Given this prediction, an estimate of the original image can be recovered by:

$$\hat{\mathbf{x}}_0 = \frac{1}{\sqrt{\alpha_t}} (\mathbf{x}_t - \sqrt{1 - \alpha_t} \epsilon_\theta(\mathbf{x}_t, t)). \quad (2)$$

By reversing the noising process across all timesteps, the model gradually transforms random noise into a clean sample. This framework forms the basis for many recent advances in generative modeling across images, video, and beyond. However, this iterative denoising process incurs significant computational cost during inference, making real-time generation challenging.

**Diffusion Transformer.** The Diffusion Transformer (DiT) is a recently proposed architecture that replaces the traditional U-Net backbone with a Transformer-based design, offering improved scalability and expressiveness. A typical DiT model consists of a sequence of Transformer blocks  $\{g^b\}_{b=1}^B$ , where  $B$  is the number of blocks. Each Transformer block  $g^b$  can be expressed as a composition of three modules:

$$g^b = \mathcal{F}_{SA}^b \circ \mathcal{F}_{CA}^b \circ \mathcal{F}_{FF}^b, \quad (3)$$

where  $\mathcal{F}_{SA}^b$ ,  $\mathcal{F}_{CA}^b$ , and  $\mathcal{F}_{FF}^b$  denote the self-attention, cross-attention, and feed-forward submodules in the  $b$ -th block, respectively. As the model progresses through the reverse process, these features are continuously updated, reflecting the model's step-wise refinement of the generated sample.

**TaylorSeer.** Previous feature caching methods accelerate inference by reusing the same features across an interval of timesteps. Specifically, given an interval  $\{t, t-1, \dots, t-N+1\}$ , they compute  $\mathcal{F}(\mathbf{x}_t)$  once and approximate the rest as:  $\mathcal{F}(\mathbf{x}_{t-k}) \approx \mathcal{F}(\mathbf{x}_t)$ , for  $k = 1, \dots, N-1$ . This direct reuse strategy, while efficient,

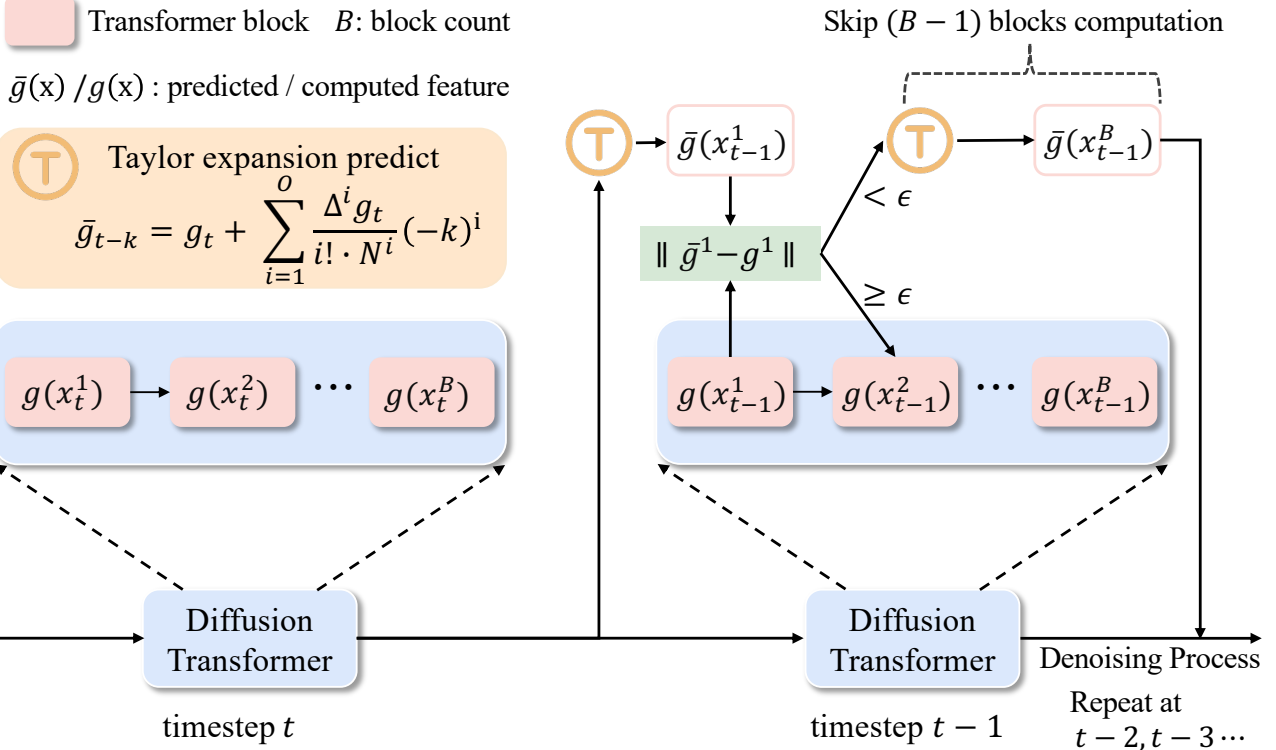


Figure 2. The framework of our method. At each timestep  $t$ , we first compute the actual output of the first block and simultaneously predict it using Taylor expansion. The prediction error is then evaluated. If the error is below a threshold  $\epsilon$ , indicating that the Taylor prediction is reliable, we use it to approximate the last block feature-skipping the computation of the remaining  $B - 1$  blocks to accelerate inference. Otherwise, we fall back to full computation of all blocks. This process is repeated for each subsequent timestep.

leads to increasing approximation error as the time gap widens. To address this, TaylorSeer [15] proposed to predict features rather than reuse them verbatim. Motivated by the observation that features and their derivatives evolve smoothly over timesteps, TaylorSeer applies Taylor series expansions using cached multi-order differences to capture the temporal dynamics of features. This method enables more accurate estimation of future features in a non-parametric manner. At timestep  $t$ , they defined a cache storing the feature and its  $O$ -th order finite differences:

$$\mathcal{C}(x_t^b) := \{\mathcal{F}(x_t^b), \Delta\mathcal{F}(x_t^b), \dots, \Delta^O\mathcal{F}(x_t^b)\}, \quad (4)$$

where  $\mathcal{F}(x_t^b)$  denotes features at fully activated timesteps and  $\Delta^i\mathcal{F}(x_t^b)$  represents the  $i$ -th order finite difference. To avoid explicit computation, they approximated higher-order derivatives using finite differences. Then the features for the  $t - k$  steps are predicted as:

$$\bar{\mathcal{F}}(x_{t-k}^b) = \mathcal{F}(x_t^b) + \sum_{i=1}^O \frac{\Delta^i \mathcal{F}(x_t^b)}{i! \cdot N^i} (-k)^i. \quad (5)$$

### 3.2. Last Block Forecast

In TaylorSeer, each prediction unit is defined at the module level. That is, for every module within each transformer block, TaylorSeer stores intermediate features and their finite differences during inference to perform Taylor expansion. However, modern DiT architectures typically contain a large number of modules—often exceeding 100—resulting in substantial computational and memory overhead. Specifically, storing and predicting features for all modules incurs a cost proportional to almost  $3 \times B \times O$ .

TaylorSeer revealed that intermediate features across blocks are highly predictable. Given the strictly sequential nature of DiT, where each block passes information to the next, we think that it is reasonable and feasible to accelerate the process by predicting the output of the last block. Based on this, we propose a **Last Block Forecast** strategy: instead of applying the Taylor predictor to every module’s intermediate features, we apply it directly to the last block at each timestep. Formally, given the last block feature  $g(x_t^B)$  at timestep  $t$ , we cache the following features and finite differences:

$$\mathcal{C}(x_t^B) := \{g(x_t^B), \Delta g(x_t^B), \dots, \Delta^O g(x_t^B)\}. \quad (6)$$

Then, we estimate future outputs for the  $t - k$  step using a Taylor expansion:

$$\bar{g}(x_{t-k}^B) = g(x_t^B) + \sum_{i=1}^O \frac{\Delta^i g(x_t^B)}{i! \cdot N^i} (-k)^i. \quad (7)$$

The Last Block Forecast strategy reduces the caching requirement from  $3 \times B \times O$  features to just  $O$ , significantly lowering both memory usage and prediction time. Moreover, it enables efficient acceleration while preserving the benefits of higher-order approximation, making it particularly suitable for large-scale DiT models.

### 3.3. Prediction Confidence Gating

While the last block forecast reduces the overhead of feature caching and prediction, the design where TaylorSeer adopted a fixed caching schedule during inference can still lead to quality degradation, especially when the predicted feature significantly deviates from the true feature. Therefore, it is critical to determine *when* to trust the Taylor predictor and *when* to fall back to actual computation.

We discover that Transformer-based architectures like DiT, the blocks exhibit strong sequential dependencies—meaning the quality of early block predictions often reflects the predictability of later blocks. Motivated by this insight, we introduce a lightweight proxy estimation method, Prediction Confidence Gating (PCG), which uses the prediction error of the first block to estimate the reliability of Taylor-based prediction at the current timestep (Figure 2). Specifically, at each timestep  $t - k$ , we apply Taylor expansion to predict the first Transformer block output, using the same expansion form defined in Eq. 7, but applied at the first block:

$$\bar{g}(x_{t-k}^1) = g(x_t^1) + \sum_{i=1}^O \frac{\Delta^i g(x_t^1)}{i! \cdot N^i} (-k)^i. \quad (8)$$

Meanwhile, we also compute the full output of the first block, denoted as  $g(x_{t-k}^1)$ , at each timestep. We compare this output with the corresponding Taylor-predicted result using a predefined error metric:

$$\frac{\|\bar{g}(x_{t-k}^1) - g(x_{t-k}^1)\|}{\|g(x_{t-k}^1)\|} < \epsilon. \quad (9)$$

If the approximation error is below a threshold  $\epsilon$ , we consider the Taylor expansion reliable at this timestep. In this case, we allow the Taylor-predicted features to estimate the output of the last transformer block. Otherwise, we fall back to full computation: This strategy allows us to dynamically adapt the use of Taylor-based prediction, ensuring that inference speedup does not come at the cost of significant quality degradation. Since the first block is shallow and fast to compute, the overhead of this additional check is minimal.

## 4. Experiments

### 4.1. Experiment Settings

**Model Configurations.** To validate the generality of our method across diverse generative settings, we evaluate it on three representative diffusion models spanning different modalities and resolutions. FLUX.1-dev [10], a text-to-image model, produces high-resolution outputs of 1024×1024 using the Rectified Flow sampler [16]. DiT-XL/2 [23], a class-conditional image generator, follows a 50-step DDIM [30] schedule to generate 256×256 images. Meanwhile, Wan Video [33], designed for text-to-video generation, synthesizes 81-frame clips at 480×832 resolution, adhering to its original sampling configuration. This diverse selection of models ensures a comprehensive evaluation of both inference efficiency and generation quality. FLUX and Wan models are implemented in the Paddlepaddle [21] framework, while DiT is implemented using PyTorch [22]. To ensure fairness and compatibility, our acceleration method is integrated into each model’s original inference pipeline without altering their underlying architecture or training setup. All experiments are conducted on NVIDIA A800 80GB GPUs, and latency is measured under consistent hardware and software conditions.

**Evaluation and Metrics.** We evaluate the effectiveness of our method from two perspectives: acceleration and visual quality. Our experimental setup closely follows the configurations of TaylorSeer [15] and TeaCache [13] to ensure fair comparison. To assess inference efficiency, we uniformly report inference latency and Floating Point Operations (FLOPs) as the primary metric. For generation quality, we incorporate task-specific evaluation metrics tailored to each generation setting. For text-to-image generation, we adopt the DrawBench benchmark [27] and evaluate the results using ImageReward [37], which estimates alignment with human preferences. Furthermore, we use PSNR and SSIM to quantify the similarity between outputs produced by our accelerated method and those generated by the original models for text-to-image generation on the COCO-1K dataset. For class-conditional image generation, we employ the FID-50k [5], sFID-50k, and Inception Score, which measures the distributional similarity between generated samples and real training data. For text-to-video generation, we use VBFench [8], a video-specific benchmark containing 946 prompts, designed to reflect human-aligned quality judgments. In addition to ImageReward, we further report PSNR, SSIM, and LPIPS [42] to assess the perceptual and structural similarity between videos generated by different methods.

### 4.2. Text-to-image model

**Quantitative Study.** We evaluate our method under two different settings and compare it with prior works, including

Table 1. Quantitative comparison of our method and baselines on the FLUX model for text-to-image generation.

Method	Acceleration			Visual Quality		
	FLOPs(T)↓	Latency(s)↓	Speed↑	Image Reward↑	SSIM ↑	PSNR↑
FLUX.1 [10]						
dev 50steps	1910.10	23.23	1.00x	1.0398	-	-
PAB [43]	1169.60	14.80	1.57x	1.0006	0.8494	24.65
Teocache ( $\delta=0.25$ ) [13]	1069.84	13.55	1.71x	1.0039	0.806	22.13
Taylorseer ( $N=2, O=1$ ) [15]	993.53	13.56	1.71x	1.0005	0.850	24.02
Ours ( $\epsilon=0.03$ )	<b>826.82</b>	<b>11.26</b>	<b>2.06x</b>	<b>1.0398</b>	<b>0.937</b>	<b>29.42</b>
Teocache ( $\delta=0.40$ ) [13]	802.48	10.14	2.29x	0.9889	0.716	19.26
Taylorseer ( $N=5, O=2$ ) [15]	<b>458.86</b>	8.21	2.83x	0.9793	0.648	17.40
Ours ( $\epsilon=0.13$ )	503.72	<b>7.19</b>	<b>3.13x</b>	<b>0.9956</b>	<b>0.813</b>	<b>22.00</b>

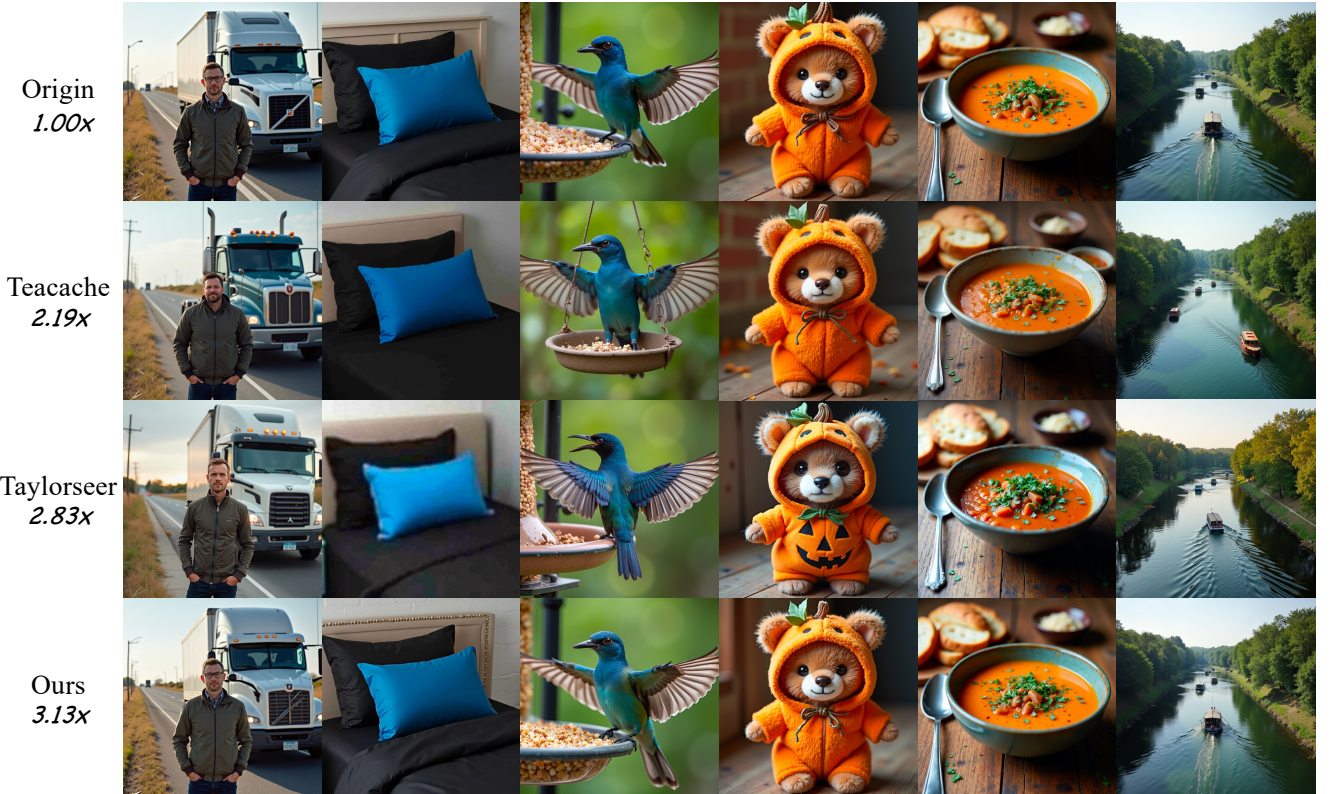


Figure 3. Visualization of different acceleration methods on FLUX. Our method achieves higher visual quality and greater similarity to the original image while operating at a faster speed.

PAB [43], Teocache [13], and TaylorSeer [15]. As shown in Table 1, our approach achieves the best trade-off between inference efficiency and generation quality in both settings. Under the low acceleration setting, our method achieves the fastest latency of 11.26s, representing a 2.06x speedup, while also attaining the highest Image Reward (1.0398) and SSIM (0.937), with PSNR (29.42)—substantially outperforming other baselines. Importantly, under this acceleration setting, the Image Reward score remains identical to that of the original model, demonstrating that our method preserves generation quality without compromise. In the more aggressive setting, our method further reduces latency to 7.19s, with a 3.13x speedup, maintaining competitive visual quality (Image Reward 0.9956, SSIM 0.813, PSNR 22.00). Compared to TaylorSeer [15], our method achieves a latency reduction of 1.02 seconds, while simultaneously

preserving generation quality. This demonstrates the effectiveness of our proposed method in achieving a better trade-off between inference efficiency and generation quality.

Table 2. Quantitative comparison of our method and baselines on the DiT model for class-to-image generation.

Method	Effcient	Acceleration			Visual Quality			
		Attention [4]	FLOPs(T)↓	Latency(s)↓	Speed↑	FID↓	sFID↓	Inception Score↑
DiT [23]								
ori 50steps	✓		23.74	0.428	1.00x	2.32	4.32	241.25
ori 20 steps	✓		9.49	0.191	2.24x	3.18	5.15	221.43
FORA ( $N = 3$ ) [28]	✓		8.58	0.197	2.17x	3.55	6.36	229.02
ToCa ( $N = 3$ ) [50]	✗		10.23	0.216	1.98x	2.87	4.76	235.21
DuCa ( $N = 3$ ) [49]	✓		9.58	0.208	2.06x	2.88	4.66	233.37
Taylorseer ( $N = 3, O = 3$ ) [15]	✓		8.56	0.248	1.73x	2.34	4.69	<b>238.42</b>
Ours ( $\epsilon=0.08$ )	✓		12.86	<b>0.181</b>	<b>2.36x</b>	<b>2.34</b>	<b>4.28</b>	235.76

improving SSIM by 25.5% and PSNR by 26.4%.

**Qualitative Study.** Figure 3 shows that our method preserves high image quality even under accelerated inference. The generated images retain the essential subjects and background elements from the original outputs. In contrast, other methods often yield blurry results or common-sense inconsistencies, such as lamps appearing on rooftops, an incomplete truck in Teacache [13], or a fuzzy bed in Taylorseer [15]. These results highlight our method’s ability to achieve a better trade-off between inference speed and visual fidelity.

### 4.3. Class-to-Image model

**Quantitative Study.** To further validate the generality of our method, we conduct experiments on DiT using various baseline acceleration strategies. As shown in Table 2, our method offers a superior balance between inference speed and visual quality. Specifically, our method attains the fastest inference latency (0.181s) and the highest speed-up ratio (2.36x) while preserving visual quality comparable to the original 50-step generation. In terms of quality metrics, we achieve an FID of 2.34, sFID of 4.28, outperforming most efficient baselines such as FORA [28], ToCa [50], and DuCa [49]. Notably, although TaylorSeer achieves a slightly lower FLOPs count, it suffers from higher latency due to its module-wise prediction overhead. In contrast, our method applies a lightweight last block forecast and a dynamic gating mechanism, resulting in lower runtime overhead without sacrificing fidelity. In addition, our method preserves efficient attention mechanisms [4] throughout, ensuring compatibility with common lightweight DiT backbones.

### 4.4. Text-to-Video model

**Quantitative Study.** Quantitative results on the Wan Video model are shown in Table 3. Our method achieves the highest inference speed, with a latency of only 40.02 seconds, representing a 4.14x acceleration over the original 50-step baseline (165.69s). Notably, this speedup outperforms all other training-free acceleration methods, including Te-

cache(3.83x) [13] and Taylorseer(3.66x) [15], while also offering superior visual quality. Specifically, our approach maintains a VBench score of 79.01%, just 1.3% below the original unaccelerated baseline (80.31%), yet significantly higher than PAB (71.86%) [43], Teacache (75.39%) [13], and TaylorSeer (76.68%) [15]. In terms of perceptual quality, our method achieves the best SSIM (0.5495) and PSNR (16.04), which outperform TaylorSeer by 63.5% and 31.6% respectively, demonstrating that our adaptive caching mechanism helps reduce approximation errors and better preserve visual details. These results suggest that our method not only enables the highest acceleration but also minimizes quality degradation, effectively balancing speed and fidelity.

### 4.5. Ablation Study

**Performance of Different Prediction Confidence Threshold  $\epsilon$ :** Figure 1 plots the speed-quality trade-off of our method as the confidence threshold  $\epsilon$  varies ( $\epsilon \in 0.13, 0.30, 0.50, 0.80$ ). As expected, larger thresholds admit more aggressive reuse and thus yield higher speed-up ratios. Although image-quality metrics (VBench, SSIM, PSNR) gradually decline with increasing  $\epsilon$ , our curves remain above those of all baselines at comparable speeds, indicating a slower quality-decay rate. The advantage is most pronounced relative to PAB: once PAB approaches a 2x speed-up, its quality drops sharply, whereas our method still delivers substantially higher fidelity. These results confirm that the Prediction Confidence Gating mechanism provides a flexible knob for trading speed for quality while preserving a consistently better balance than competing approaches.

**Effectiveness of each Component.** To evaluate the effectiveness of each component in our method, we conduct an ablation study focusing on two key modules: Last Block Forecast and Prediction Confidence Gating (PCG), as shown in Table 4. To ensure fairness, we keep the TaylorSeer-related configurations consistent across all variants, applying the same Taylor order and caching intervals when applicable.

Table 3. Quantitative comparison of our method and baselines on the Wan model for text-to-video generation.

Method	Acceleration		Visual Quality			
	Latency(s)↓	Speed↑	VBench(%)↑	SSIM ↑	PSNR↑	LPIPS ↓
Wan Video [33]						
ori 50steps	165.69	1.00x	80.31	-	-	-
PAB [43]	78.02	2.12x	71.86	0.4162	15.9141	0.5074
Teocache ( $\delta = 0.26$ ) [13]	43.25	3.83x	75.39	0.3398	12.1620	0.6275
Taylorseer ( $N = 5, O = 1$ ) [15]	45.27	3.66x	76.68	0.3338	12.1926	0.5902
Ours ( $\epsilon = 0.13$ )	<b>40.02</b>	<b>4.14x</b>	<b>79.01</b>	<b>0.5495</b>	<b>16.0418</b>	<b>0.3185</b>

Table 4. Ablation study of each component in our method on the FLUX model for text-to-image generation.

Forecast level	PCG	Latency(s)↓	PSNR↑	Image Reward↑	SSIM ↑	Memory Usage (GB)↓
module	✗	13.56	24.02	1.0005	0.850	39.69
last block	✗	12.41	24.00	1.0109	0.849	<b>35.73</b>
last block	✓	<b>11.26</b>	<b>29.42</b>	<b>1.0398</b>	<b>0.937</b>	35.78

When the forecast level is set to module, the method corresponds to the original TaylorSeer. Switching to the Last Block Forecast reduces latency from 13.56s to 12.41s, while maintaining nearly the same visual quality—SSIM drops only marginally from 0.850 to 0.849, and PSNR from 24.02 to 24.00. Notably, ImageReward slightly improves from 1.0005 to 1.0109, suggesting that our Last Block Forecast effectively eliminates redundant intermediate predictions without degrading generation quality. With both the Last Block Forecast and PCG enabled, the visual quality improves substantially. Despite achieving even faster inference (latency reduced by 1s compared to Last Block Forecast-only), SSIM rises to 0.937 and PSNR reaches 29.42—a relative improvement of 22.58%. ImageReward also increases from 1.0109 to 1.0398. These results demonstrate that PCG enables a better trade-off between speed and image quality. We also evaluate the peak GPU memory usage during inference. Our method reduces GPU memory consumption by approximately 10% (from 39.69 GB to 35.78 GB), which is particularly beneficial for large-scale DiT models.

**Analysis of the Prediction Confidence Gating.** To examine whether the first-block error is a reliable proxy for the accuracy of the last-block Taylor prediction, we plot the per-timestep errors defined in Eq.9 in Figure 4. The scatter plot reveals a clear positive correlation: when the Taylor error of the first block is small, the error of the last block output is likewise small, and vice versa. This strong coupling confirms the effectiveness of our Prediction Confidence Gating (PCG). By invoking Taylor prediction only when the first-block error is low—and reverting to standard

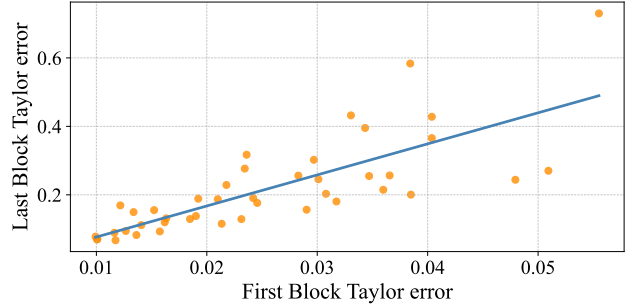


Figure 4. Correlation between the first block and the last block Taylor errors.

computation otherwise—PCG exploits Taylor’s speed advantage whenever it is trustworthy while sidestepping cases that would degrade quality.

## 5. Conclusion

We propose a training-free framework to accelerate diffusion model inference by leveraging the predictive power of Taylor expansion more effectively. Unlike prior methods that rely on fixed reuse patterns and module-level predictions, our approach introduces a last block forecast strategy to reduce memory and computation, and a prediction confidence gating mechanism that dynamically decides when to trust Taylor-based approximations. Experiments on multiple models demonstrate that our method achieves superior speed-quality trade-offs, offering faster generation with minimal quality degradation. We believe our findings shed light on the importance of dynamic control and last block

approximation in efficient diffusion inference. This paves the way for acceleration strategies that are more practical and adaptive in real-world applications.

## Acknowledgments

This work was supported by the Key Research and Development Program of Yunnan Province under Grant No. 202403AA080002

## References

- [1] Andreas Blattmann, Tim Dockhorn, Sumith Kulal, Daniel Mendelevitch, Maciej Kilian, Dominik Lorenz, Yam Levi, Zion English, Vikram Voleti, Adam Letts, et al. Stable video diffusion: Scaling latent video diffusion models to large datasets. *arXiv*, 2023. [2](#)
- [2] Pengtao Chen, Mingzhu Shen, Peng Ye, Jianjian Cao, Chongjun Tu, Christos-Savvas Bouganis, Yiren Zhao, and Tao Chen. *delta-dit*: A training-free acceleration method tailored for diffusion transformers. *arXiv*, 2024. [2](#), [3](#)
- [3] Xinle Cheng, Zhuoming Chen, and Zhihao Jia. Cat pruning: Cluster-aware token pruning for text-to-image diffusion models. *arXiv*, 2025. [2](#), [3](#)
- [4] Tri Dao, Dan Fu, Stefano Ermon, Atri Rudra, and Christopher Ré. Flashattention: Fast and memory-efficient exact attention with io-awareness. *NeurIPS*, 35:16344–16359, 2022. [7](#)
- [5] Martin Heusel, Hubert Ramsauer, Thomas Unterthiner, Bernhard Nessler, and Sepp Hochreiter. Gans trained by a two time-scale update rule converge to a local nash equilibrium. *NeurIPS*, 30, 2017. [5](#)
- [6] Jonathan Ho, Ajay Jain, and Pieter Abbeel. Denoising diffusion probabilistic models. *NeurIPS*, 33:6840–6851, 2020. [1](#), [3](#)
- [7] Zhiping Hu, Hao Yan, Kuihua Huang, Jincai Huang, Zhong Liu, and Changjun Fan. Dtiu: A self-supervised grid-enhanced diffusion model for trajectory imputation in unconstrained scenarios. *KBS*, page 113848, 2025. [2](#)
- [8] Ziqi Huang, Yinan He, Jiashuo Yu, Fan Zhang, Chenyang Si, Yuming Jiang, Yuanhan Zhang, Tianxing Wu, Qingyang Jin, Nattapol Chanpaisit, et al. Vbench: Comprehensive benchmark suite for video generative models. In *CVPR*, pages 21807–21818, 2024. [5](#)
- [9] Minchul Kim, Shangqian Gao, Yen-Chang Hsu, Yilin Shen, and Hongxia Jin. Token fusion: Bridging the gap between token pruning and token merging. In *WACV*, pages 1383–1392, 2024. [2](#), [3](#)
- [10] Black Forest Labs. Flux. <https://github.com/black-forest-labs/flux>, 2024. [5](#), [6](#)
- [11] Yanyu Li, Huan Wang, Qing Jin, Ju Hu, Pavlo Chemerys, Yun Fu, Yanzhi Wang, Sergey Tulyakov, and Jian Ren. Snap-fusion: Text-to-image diffusion model on mobile devices within two seconds. *NeurIPS*, 36:20662–20678, 2023. [2](#), [3](#)
- [12] Yunxiang Li, Xianghao Kong, Jiacheng Xie, Greg Ver Steeg, and You Zhang. Denoising diffusion wavelet models for zero-shot medical image translation. *KBS*, page 113800, 2025. [2](#)
- [13] Feng Liu, Shiwei Zhang, Xiaofeng Wang, Yujie Wei, Haonan Qiu, Yuzhong Zhao, Yingya Zhang, Qixiang Ye, and Fang Wan. Timestep embedding tells: It's time to cache for video diffusion model. In *CVPR*, pages 7353–7363, 2025. [3](#), [5](#), [6](#), [7](#), [8](#)
- [14] Haozhe Liu, Wentian Zhang, Jinheng Xie, Francesco Faccio, Mengmeng Xu, Tao Xiang, Mike Zheng Shou, Juan-Manuel Perez-Rua, and Jürgen Schmidhuber. Faster diffusion via temporal attention decomposition. *TMLR*, 2024. [3](#)
- [15] Jiacheng Liu, Chang Zou, Yuanhuiyi Lyu, Junjie Chen, and Linfeng Zhang. From reusing to forecasting: Accelerating diffusion models with taylorseers. *ICCV*, 2025. [2](#), [3](#), [4](#), [5](#), [6](#), [7](#), [8](#)
- [16] Xingchao Liu, Chengyue Gong, and Qiang Liu. Flow straight and fast: Learning to generate and transfer data with rectified flow. *ICLR2023*, 2022. [5](#)
- [17] Cheng Lu, Yuhao Zhou, Fan Bao, Jianfei Chen, Chongxuan Li, and Jun Zhu. Dpm-solver: A fast ode solver for diffusion probabilistic model sampling in around 10 steps. *NeurIPS*, 35:5775–5787, 2022. [2](#)
- [18] Cheng Lu, Yuhao Zhou, Fan Bao, Jianfei Chen, Chongxuan Li, and Jun Zhu. Dpm-solver++: Fast solver for guided sampling of diffusion probabilistic models. *MIR*, pages 1–22, 2025. [2](#)
- [19] Xinyin Ma, Gongfan Fang, and Xinchao Wang. Deepcache: Accelerating diffusion models for free. In *CVPR*, pages 15762–15772, 2024. [2](#), [3](#)
- [20] Xin Ma, Yaohui Wang, Gengyun Jia, Xinyuan Chen, Ziwei Liu, Yuan-Fang Li, Cunjian Chen, and Yu Qiao. Latte: Latent diffusion transformer for video generation. *TMLR*, 2024. [2](#)
- [21] Yanjun Ma, Dianhai Yu, Tian Wu, and Haifeng Wang. Padlepaddle: An open-source deep learning platform from industrial practice. *Frontiers of Data and Domputing*, 1(1): 105–115, 2019. [5](#)
- [22] Adam Paszke, Sam Gross, Francisco Massa, Adam Lerer, James Bradbury, Gregory Chanan, Trevor Killeen, Zeming Lin, Natalia Gimelshein, Luca Antiga, et al. Pytorch: An imperative style, high-performance deep learning library. *NeurIPS*, 32, 2019. [5](#)
- [23] William Peebles and Saining Xie. Scalable diffusion models with transformers. In *ICCV*, pages 4195–4205, 2023. [2](#), [3](#), [5](#), [7](#)
- [24] Aditya Ramesh, Prafulla Dhariwal, Alex Nichol, Casey Chu, and Mark Chen. Hierarchical text-conditional image generation with clip latents. *arXiv*, 1(2):3, 2022. [2](#), [3](#)
- [25] Robin Rombach, Andreas Blattmann, Dominik Lorenz, Patrick Esser, and Björn Ommer. High-resolution image synthesis with latent diffusion models. In *CVPR*, pages 10684–10695, 2022. [3](#)
- [26] Olaf Ronneberger, Philipp Fischer, and Thomas Brox. U-net: Convolutional networks for biomedical image segmentation. In *MICCAI*, pages 234–241. Springer, 2015. [1](#)
- [27] Chitwan Saharia, William Chan, Saurabh Saxena, Lala Li, Jay Whang, Emily L Denton, Kamyar Ghasemipour,

Raphael Gontijo Lopes, Burcu Karagol Ayan, Tim Salimans, et al. Photorealistic text-to-image diffusion models with deep language understanding. *NeurIPS*, 35:36479–36494, 2022. [2](#), [3](#), [5](#)

[28] Pratheba Selvaraju, Tianyu Ding, Tianyi Chen, Ilya Zharkov, and Luming Liang. Fora: Fast-forward caching in diffusion transformer acceleration. *arXiv*, 2024. [2](#), [3](#), [7](#)

[29] Jascha Sohl-Dickstein, Eric Weiss, Niru Maheswaranathan, and Surya Ganguli. Deep unsupervised learning using nonequilibrium thermodynamics. In *ICML*, pages 2256–2265. pmlr, 2015. [1](#), [3](#)

[30] Jiaming Song, Chenlin Meng, and Stefano Ermon. Denoising diffusion implicit models. *ICLR*, 2021. [3](#), [5](#)

[31] Yang Song and Stefano Ermon. Generative modeling by estimating gradients of the data distribution. *NeurIPS*, 32, 2019. [1](#)

[32] Yang Song, Prafulla Dhariwal, Mark Chen, and Ilya Sutskever. Consistency models. *arXiv*, 2023. [3](#)

[33] Team Wan, Ang Wang, Baole Ai, Bin Wen, Chaojie Mao, Chen-Wei Xie, Di Chen, Feiwu Yu, Haiming Zhao, Jianxiao Yang, et al. Wan: Open and advanced large-scale video generative models. *arXiv*, 2025. [5](#), [8](#)

[34] Shuo Wang, Shuzhen Xu, Cuicui Lv, Chaoqing Ma, and Fangbo Cai. Diff-reformer: A diffusion-augmented recursive context transformer for image super-resolution. *KBS*, page 113758, 2025. [2](#)

[35] Yachuan Wang, Bin Zhang, and Hao Yuan. Cymodiff: Dimensional cycle diffusion for unsupervised 2d-to-3d motion retargeting. *KBS*, page 113568, 2025. [2](#)

[36] Yujie Wei, Shiwei Zhang, Zhiwu Qing, Hangjie Yuan, Zhiheng Liu, Yu Liu, Yingya Zhang, Jingren Zhou, and Hongming Shan. Dreamvideo: Composing your dream videos with customized subject and motion. In *CVPR*, pages 6537–6549, 2024. [3](#)

[37] Jiazheng Xu, Xiao Liu, Yuchen Wu, Yuxuan Tong, Qinkai Li, Ming Ding, Jie Tang, and Yuxiao Dong. Imagereward: Learning and evaluating human preferences for text-to-image generation. *NeurIPS*, 36:15903–15935, 2023. [5](#)

[38] Zhuoyi Yang, Jiayan Teng, Wendi Zheng, Ming Ding, Shiyu Huang, Jiazheng Xu, Yuanming Yang, Wenyi Hong, Xiaohan Zhang, Guanyu Feng, et al. Cogvideox: Text-to-video diffusion models with an expert transformer. *ICLR*, 2024. [2](#)

[39] Chengsheng Yuan, Jingfa Pang, Jianwei Fei, Xinting Li, and Zhihua Xia. At-diff: An adversarial diffusion model for unrestricted adversarial examples generation. *KBS*, page 113645, 2025. [2](#)

[40] Hansheng Zeng, Yuqi Li, Ruize Niu, Chuanguang Yang, and Shiping Wen. Enhancing spatiotemporal prediction through the integration of mamba state space models and diffusion transformers. *KBS*, 316:113347, 2025. [2](#)

[41] Evelyn Zhang, Bang Xiao, Jiayi Tang, Qianli Ma, Chang Zou, Xuefei Ning, Xuming Hu, and Linfeng Zhang. Token pruning for caching better: 9 times acceleration on stable diffusion for free. *arXiv*, 2024. [2](#), [3](#)

[42] Richard Zhang, Phillip Isola, Alexei A Efros, Eli Shechtman, and Oliver Wang. The unreasonable effectiveness of deep features as a perceptual metric. In *CVPR*, pages 586–595, 2018. [5](#)

[43] Xuanlei Zhao, Xiaolong Jin, Kai Wang, and Yang You. Real-time video generation with pyramid attention broadcast. *ICLR*, 2025. [3](#), [6](#), [7](#), [8](#)

[44] Kaiwen Zheng, Cheng Lu, Jianfei Chen, and Jun Zhu. Dpm-solver-v3: Improved diffusion ode solver with empirical model statistics. *NeurIPS*, 36:55502–55542, 2023. [2](#)

[45] Zangwei Zheng, Xiangyu Peng, Tianji Yang, Chenhui Shen, Shenggui Li, Hongxin Liu, Yukun Zhou, Tianyi Li, and Yang You. Open-sora: Democratizing efficient video production for all. *arXiv*, 2024. [2](#)

[46] Haowei Zhu, Dehua Tang, Ji Liu, Mingjie Lu, Jintu Zheng, Jinzhang Peng, Dong Li, Yu Wang, Fan Jiang, Lu Tian, et al. Dip-go: A diffusion pruner via few-step gradient optimization. *NeurIPS*, 37:92581–92604, 2024. [2](#), [3](#)

[47] Jiaming Zhu, Dezhli Liu, Huayou Chen, Jinpei Liu, and Zhifu Tao. Dtsformer: Decoupled temporal-spatial diffusion transformer for enhanced long-term time series forecasting. *KBS*, 309:112828, 2025. [3](#)

[48] Jianzhi Zhuang, Jin Li, Chenjunhao Shi, Xinyi Lin, and Yang-Geng Fu. Enhanced graph transformer: Multi-scale attention with heterophilous curriculum augmentation. *KBS*, 309:112874, 2025. [2](#)

[49] Chang Zou, Evelyn Zhang, Runlin Guo, Haohang Xu, Conghui He, Xuming Hu, and Linfeng Zhang. Accelerating diffusion transformers with dual feature caching. *arXiv*, 2024. [2](#), [3](#), [7](#)

[50] Chang Zou, Xuyang Liu, Ting Liu, Siteng Huang, and Linfeng Zhang. Accelerating diffusion transformers with token-wise feature caching. *ICLR*, 2025. [2](#), [3](#), [7](#)